Research Article | Vol. 27, No. 24 / 25 November 2019 / Optics Express 35856

Optics EXPRESS

Effect of the buffer gases on the light shift suppression possibility

M. I. Vaskovskaya,[1,2] E. A. Tsygankov,[1,3] D. S. Chuchelov,[1] S. A. Zibrov,[1] V. V. Vassiliev,[1] and V. L. Velichansky[1]

[1]The Lebedev Physical Institute of the Russian Academy of Sciences, Moscow 119991, Russia
[2]vaskovskayami@lebedev.ru
[3]selentinthebright@gmail.com

Abstract: We theoretically and experimentally demonstrate that the light shift of the coherent population trapping resonance frequency depends on the buffer gases pressure. The light shift suppression becomes impossible when a certain value of the buffer gases pressure is exceeded. We estimate the minimal dimensions of an atomic cell at which the zero light shift and the lowest ground-state relaxation rate can be achieved simultaneously. A new technique of the light shift cancellation by means of a feedback utilizing the RF power modulation is proposed.

1. Introduction

The coherent population trapping (CPT) phenomenon has been used in many applications since the first experimental observations in the late 70s [1–4]. One of them is the CPT-based clocks, which allows a significant reduction in the size of the microwave frequency standards while maintaining high Q-factor of the metrological resonance. Technological advances, such as vertical-cavity surface-emitting lasers (VCSELs) and micro-fabricated (MEMS) atomic vapor cells, have allowed to develop compact and chip-scale CPT-based atomic clocks [5–7].

The clock frequency stability depends on the characteristics of the CPT resonance, especially on it's contrast and width [8]. In practice, the long-term frequency stability is mainly limited by changes of the optical field intensity if the light shift of the CPT resonance frequency is not suppressed [8–10] and by drift of the temperature. The standard technique to reduce the relaxation rate of the atomic ground-state coherence, on which the resonance width depends, is to fill an atomic cell with buffer gases (BG). The smaller is the cell size, the higher BG pressure is required [11–13]. By taking a specific mixture of BG with opposite signs of linear temperature coefficients the temperature influence on the resonance frequency can be reduced significantly [14]. At the same time, the proper choice of the depth of a VCSEL current modulation and the corresponding polychromatic spectrum can provide the zero light shift [15–20].

In this paper we demonstrate theoretically and experimentally that the light shift suppression possibility depends on the total BG pressure. When the pressure exceeds a certain value, none of the available spectrum of the RF modulated VCSEL can provide the zero light shift. Consequently, in atomic cells smaller than some critical size, the lowest ground-state relaxation rate and the zero light shift can not be simultaneously obtained. We also empirically estimate the critical size for the cylindrical atomic cells filled with ^{87}Rb atoms and an Ar-N_2 mixture.

2. Theory

In a chip-scale atomic clock the CPT resonance is excited by a polychromatic optical field [7], which is obtained by modulation of a VCSEL injection current. Such an optical field does not correspond to a field subjected to the frequency modulation or the amplitude modulation, or their combination [21], but for simplicity of calculation we describe it here as the following

#377671 https://doi.org/10.1364/OE.27.035856
Journal © 2019 Received 13 Sep 2019; revised 6 Nov 2019; accepted 14 Nov 2019; published 21 Nov 2019

Optics EXPRESS

phase-modulated optical field with σ_+ or σ_- polarization

$$\mathcal{E}\left(\mathbf{e_x}\cos\left[\omega t + a\sin\Omega t\right] \pm \mathbf{e_y}\sin\left[\omega t + a\sin\Omega t\right]\right), \tag{1}$$

where modulation frequency Ω is nearly equal to the half of the ground-state hyperfine frequency interval ω_g of an alkali metal atom, $\omega_g/2 = \Omega + \delta$. The CPT resonance is obtained as a dependence of the optical field absorption coefficient of an alkali metal atoms vapor on the two-photon detuning δ, wherein $\delta \ll \omega_g$. The carrier frequency ω is considered equal to the half-sum of the frequencies of the D_1 line transitions of an alkali metal atom to the upper level of the excited state $\mathbf{nP_{1/2}}$. In the case of ^{87}Rb atoms used in the experiment these transitions are $\mathbf{5S_{1/2}}\,|F = 2; m\rangle \rightarrow \mathbf{5P_{1/2}}\,|F = 2; m \pm 1\rangle$ and $\mathbf{5S_{1/2}}\,|F = 1; m\rangle \rightarrow \mathbf{5P_{1/2}}\,|F = 2; m \pm 1\rangle$, where the sign "+" corresponds to σ_+ polarization and the sign "−" corresponds to σ_- polarization. The value of quantum number m changes from −2 to 1 for the former and from −1 to 2 for the latter. As far as $e^{-i(\omega t + a\sin\Omega t)} = \sum_k J_k(a)e^{-i(\omega + k\Omega)t}$, where $J_k(a)$ is the Bessel function of the first kind, optical pumping of an atomic ensemble to the dark state is performed by the first sidebands $k = \pm 1$. On top of everything, in chip-scale clocks a magnetic field is applied to an atomic cell to shift the magneto-sensitive CPT resonances from the metrological one excited between the sublevels $\mathbf{nS_{1/2}}\,|F = I + 1/2; m = 0\rangle$ and $\mathbf{nS_{1/2}}\,|F = I - 1/2; m = 0\rangle$.

Since optical field slightly changes frequencies of the optical transitions via the AC Stark effect, the frequency interval between the ground-state sublevels $\mathbf{nS_{1/2}}\,|F = I + 1/2; m = 0\rangle$ and $\mathbf{nS_{1/2}}\,|F = I - 1/2; m = 0\rangle$ of an alkali metal atom is also perturbed. This leads to a frequency displacement δ_0 of the minimum of the metrological CPT resonance, i.e., the condition for the maximum of the optical field transmission by an atomic ensemble becomes $\delta - \delta_0 = 0$. The light shift of the CPT resonance frequency induced by the optical field (1) under standard assumptions of the low saturation regime and the resonant approximation can be treated as the algebraic sum of the light shifts induced by its individual spectrum components in the case of an optically thin medium [15,16,22]. Then, if the excited-state sublevel $\mathbf{nP_{1/2}}\,|F = I - 1/2; m = \pm 1\rangle$ and the Doppler broadening of the optical line are not taken into account, and the Doppler effect for the two-photon transition is neglected (which is cancelled due to the Dicke narrowing [23]), the total light shift is given by the following expression [24]:

$$\delta_0 = -\frac{1}{\Omega}\left(\frac{d\mathcal{E}}{2\hbar}\right)^2 \sum_k \frac{kJ_{k+1}^2(a)}{k^2 + (\Gamma/\Omega)^2} = \frac{1}{\Omega}\left(\frac{d\mathcal{E}}{2\hbar}\right)^2 \left(\frac{2}{a}\frac{\partial}{\partial a}\sum_{k=1}^{\infty} \frac{k^2 J_k^2(a)}{k^2 + (\Gamma/\Omega)^2}\right), \tag{2}$$

where Γ describes the half width at half maximum (HWHM) of the optical lines broadened via collisions of the alkali metal atoms with BG components, d is the dipole matrix element which couples the sublevels $\mathbf{nS_{1/2}}\,|F = I + 1/2; m = 0\rangle$, $\mathbf{nS_{1/2}}\,|F = I - 1/2; m = 0\rangle$ and $\mathbf{nP_{1/2}}\,|F = I + 1/2; m = \pm 1\rangle$. Expression (2) under simplifying condition $(\Gamma/\Omega)^2 \ll 1$ and taking into account the Bessel functions property $\sum_k J_k^2(a) = 1$ becomes

$$\delta_0 \simeq \frac{1}{\Omega}\left(\frac{d\mathcal{E}}{2\hbar}\right)^2 \frac{2}{a} J_0(a)J_1(a). \tag{3}$$

As formula (3) shows, the minimal modulation index when the light shift vanishes is determined by the first zero of the Bessel function $J_0(a)$, for which the index value is $a \approx 2.4$. This value of the modulation index a has the main practical interest since the Bessel function $J_1(a)$ value is smaller at values of a corresponding to all other light shift zeroes, i.e., the maximal contrast of the CPT resonance can be simultaneously obtained with the zero light shift at $a \approx 2.4$. We note that this value of the modulation index a was obtained earlier in some works via numerical calculations [15,16,25].

The situation is different when $(\Gamma/\Omega)^2$ can not be neglected compared with 1. As follows from the formula (2), the modulation index a value corresponding to the first light shift zero increases

Optics EXPRESS

with growth of Γ, while the value of a corresponding to the second light shift zero decreases, see the curve II in Fig. 1. When Γ/Ω becomes equal to ≈ 0.854, the two first points of the zero light shift merge into one, see the curve III in Fig. 1. For the case of ^{87}Rb atoms used in the experiment the corresponding value of the $\Gamma/2\pi$ is nearly 2.92 GHz. If inequality $\Gamma > 0.854\Omega$ holds, then the light shift value is greater than zero in the entire interval of a values determined by the first zero of the function $J_0(a)$ and the second zero of the function $J_1(a)$, see the curve IV in Fig. 1. This feature of the light shift dependence on a is clear: consider, for example, the hyperfine frequency light shift induced by the spectrum components $k \geq 2$ when they interact with the alkali metal atoms via sublevel $\mathbf{nP_{1/2}}\,|F = I + 1/2; m = \pm 1\rangle$. These components are detuned by $(k-1)\Omega$ and $(k+1)\Omega$ from frequencies of transitions between this excited-state sublevel and the ground-state sublevels $\mathbf{nS_{1/2}}\,|F = I - 1/2; m = 0\rangle$ and $\mathbf{nS_{1/2}}\,|F = I + 1/2; m = 0\rangle$, respectively. Therefore the light shift $\delta_{k\geq 2}$ is proportional to the following term:

$$\delta_{k\geq 2} \propto \frac{k-1}{(k-1)^2 + (\Gamma/\Omega)^2} - \frac{k+1}{(k+1)^2 + (\Gamma/\Omega)^2} \propto (k^2 - 1) - (\Gamma/\Omega)^2, \tag{4}$$

i.e., at a certain value of the total BG pressure each high-order sideband instead of decreasing the ground-state hyperfine frequency interval starts to increase it, while the low-order components $k = 0, \pm 1$ always enlarge it. For example, sign of the light shift induced by $k = 2$ component changes when $\Gamma = \sqrt{3}\Omega$; for the case of ^{87}Rb atoms used in the experiment the corresponding value of $\Gamma/2\pi$ is nearly 5.92 GHz. For completeness we note that the corresponding value of $\Gamma/2\pi$ is the same for components $k \leq -2$ due to neglect of the excited-state sublevel $\mathbf{nP_{1/2}}\,|F = I - 1/2; m = \pm 1\rangle$.

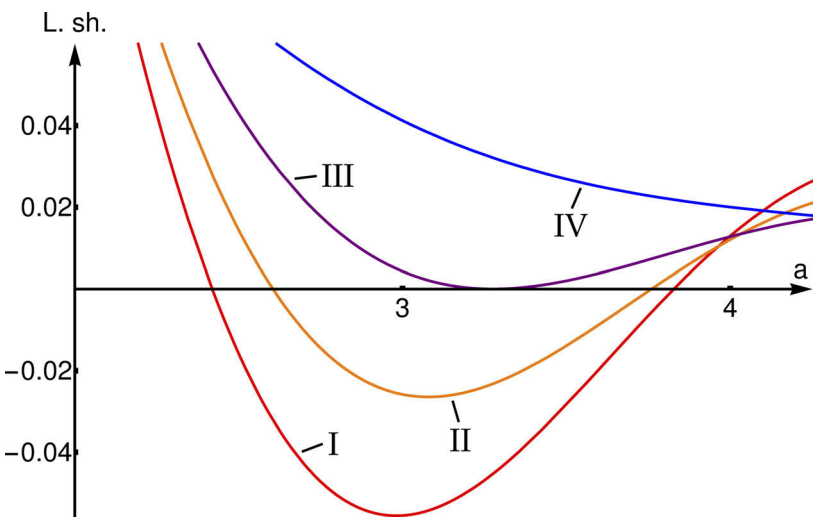

Fig. 1. Theoretical dependence of the light shift δ_0 on the modulation index a plotted via (2) for different values of the ratio Γ/Ω. $\Gamma/2\pi$ is equal to 0.5, 1.785, 2.92, and 5.92 GHz for curves I (red), II (orange), III (purple), and IV (blue), respectively, while $\Omega/2\pi$ is equal to the one half of the ^{87}Rb ground-state hyperfine frequency interval, 3.417 GHz. The vertical axis shows the light shift value in units $\frac{1}{\Omega}(d\mathcal{E}/2\hbar)^2$.

3. Experiment

The experimental setup is schematically shown in Fig. 2. A single-mode 795 nm VCSEL is current-modulated at the frequency $\Omega \approx 3.417$ GHz by a microwave synthesizer. The first-order

Optics EXPRESS

sidebands of the polychromatic spectrum (see the inset **a** in Fig. 2) excite the CPT resonance in a standard scheme using a circular polarization [7,8]. A longitudinal magnetic field (~ 0.1 G) produced by a solenoid is used to resolve the metrological "0-0" resonance. The optical signal after an atomic cell is registered by the photodetector PD_1. Coarse laser intensity control is performed by a half-wave plate and a polarizer. The beam diameter inside the cell is about 1 mm, the laser radiation power is 23 μW.

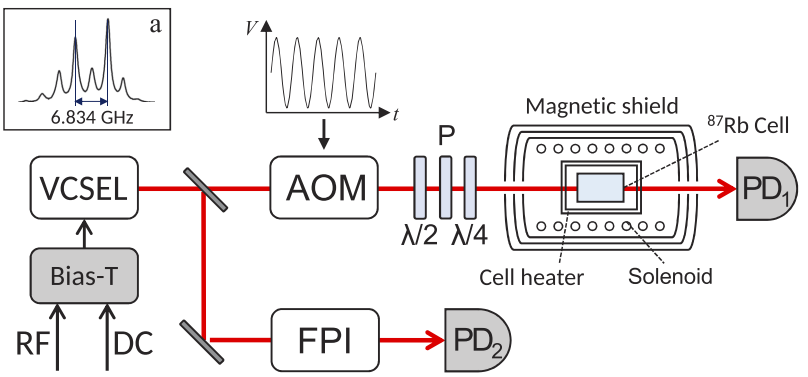

Fig. 2. The layout of experimental setup. VCSEL is a vertical-cavity surface-emitting laser tuned to ^{87}Rb D_1 line. Bias-T combines DC injection current with AC current of microwave modulation (RF). AOM is an acousto-optic modulator, FPI is a Fabry-Perot interferometer, $PD_{1,2}$ are photodetectors, $\lambda/2$ is a half-wave plate, $\lambda/4$ is a quarter-wave plate, P is a polarizer. The inset (**a**) shows a typical laser spectrum entering the atomic cell.

A set of five cylindrical cells 8 mm in diameter and 15 mm long (wall thickness is 0.7 mm) filled through a 20 mm glass-blowing stem with isotopically enriched ^{87}Rb and a mixture of Ar and N_2 is used. The values of the total BG pressure ranged from 19 to 140 Torr are shown in Table 1. The ratio of the partial pressures of gases, P_{Ar}/P_{N_2}, is 1.3 for all atomic cells. The atomic cells are produced by the glass-blowing technology. The manufacturer guarantees that the total BG pressure value and the ratio P_{Ar}/P_{N_2} differ from the declared values no more than by 5% and 3%, respectively. In order to keep the maximum of the CPT resonance amplitude, the operating temperatures for different cells range from 60 to 72 °C. A heater and a servo-loop maintain the temperature of a studied cell with an accuracy of 0.01 °C. The cell, heater and solenoid are placed inside a three-layer magnetic shield isolating the cell from the external magnetic field. The laser spectrum is registered by a scanning Fabry-Perot interferometer with a free spectral range of about 35 GHz and the photodetector PD_2.

Table 1. Characteristics of the studied cells. "Pressure" is the total pressure of BG mixture; "Optical HWHM" is the half width at half maximum of the optical absorption lines; "BG shift" is the shift of the CPT resonance frequency caused by buffer gases; "RF value of point 1 (2)" is the value of RF power, corresponding to the first (second) zero light shift point.

Atomic cell number	Pressure, Torr	Optical HWHM, GHz	BG shift, Hz	T, °C	RF value of point 1, dBm	RF value of point 2, dBm
1	19	0.43	3285	60	1.2	4.6
2	29	0.57	5452	64	1.3	4.5
3	75	1.26	14633	68	2.1	4.4
4	115	1.68	19780	71	–	–
5	140	1.96	27670	72	–	–

Optics EXPRESS

The signal registered by PD_1 is used to stabilize both the laser and the synthesizer frequencies. The laser frequency is stabilized by a servo-loop controlling the laser temperature. For stabilization of the synthesizer frequency to the maximum of the CPT resonance the frequency Ω is modulated: $\Omega(t) = \Omega + b\omega_m \cos \omega_m t$, where b is the modulation index and the typical value of ω_m is close to the HWHM of the CPT resonance. The in-phase signal produced by the lock-in amplifier is used as an error signal.

The acousto-optic modulator modulates the laser radiation intensity with a sinusoidal signal provided by the function generator (see Fig. 2). The magnitude of the light shift is proportional to the laser radiation intensity, therefore the CPT resonance frequency responds to the intensity variation. A slow sweep of the RF power with simultaneous modulation of the light intensity allows to find the RF power value at which frequency response vanishes, i.e., changes of the CPT resonance frequency due to the light intensity modulation are indistinguishable from fluctuations of the frequency caused by other factors. This point corresponds to the depth of injection current modulation at which the VCSEL's spectrum provides the zero light shift. A similar method for determination of the modulation index providing suppression of the light shift was used in [17].

Figure 3 shows dependence of the CPT resonance frequency on the RF power for the atomic cell #1. These experimental data are obtained by the aforementioned method. The RF power is scanned from −5 dBm to 6 dBm during 2860 s, while the light modulation period is 25 s (AM depth is about 30%). In this case, the servo-loops properly respond to changes in the RF power and the light intensity, and the CPT resonance frequency adiabatically follows changes in the optical field intensity.

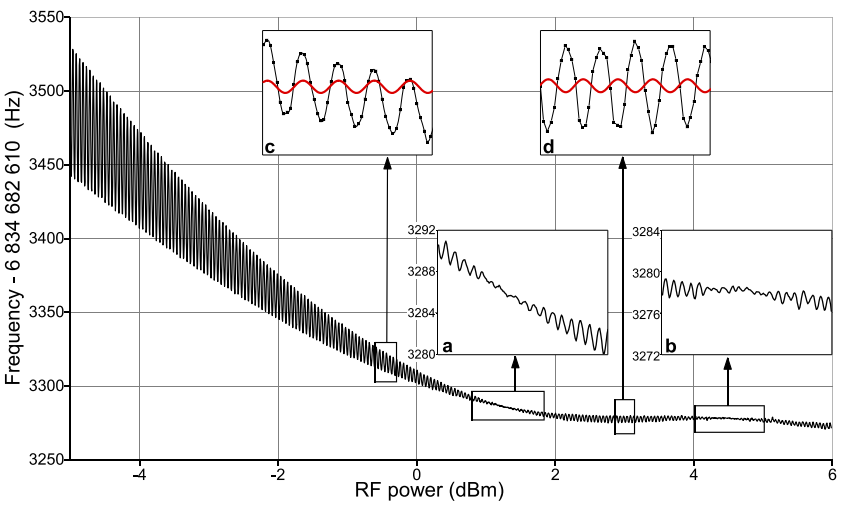

Fig. 3. Dependence of the CPT resonance frequency on the RF power with simultaneous modulation of the light intensity obtained for the atomic cell #1. Two points of the zero light shift are observed (insets **a** and **b**). Insets **c** and **d** show that the relative phase between response of the CPT resonance frequency (line marked by black squares) and the signal controlling the light intensity (red solid line) differs by π. This corresponds to the opposite sign of the light shift in these regions of dependence.

There are two RF power values at which no frequency response to the intensity modulation is observed (see insets **a** and **b** in Fig. 3). These two points divide the curve into three parts where the light shift is observed. In the left and right parts the CPT resonance frequency rises with increase of intensity (inset **c**), which means that the light shift has a positive sign. On the contrary, the light shift in the central part has a negative sign, since the resonance frequency decreases (inset **d**). The change of the shift sign confirms that the points at which the frequency

Optics EXPRESS

response vanishes correspond to the zero light shift. It should be noted that the frequencies of these points differ by about 8 Hz. This difference is discussed below.

Analogous dependencies of the CPT resonance frequency on the RF modulation power are presented in Fig. 4(a) for atomic cells #2-5. It shows that the RF modulation power required to achieve the zero light shift depends on the total BG pressure. The RF power corresponding to the first point of the zero light shift increases with pressure, while for the second point it decreases (see Table 1). For the atomic cell #4 instead of two separate points there is a range of RF power values from 2.8 dBm to 3.6 dBm in which the frequency response to the light intensity modulation for the given AM depth can not be distinguished from fluctuations of the frequency caused by other factors (in this range, the light shift is already positive, but its value is still close to zero). For the atomic cell #5 the zero light shift is not observed in the entire range of the RF power used in the experiment.

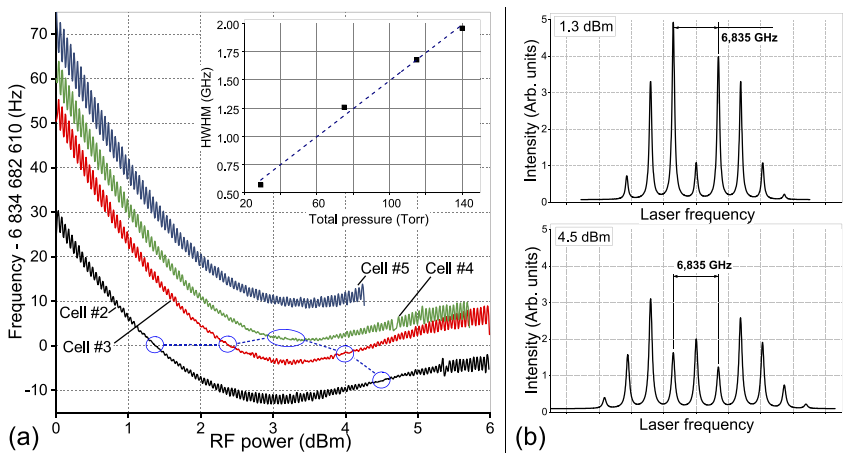

Fig. 4. (a) Dependencies of the CPT resonance frequency on the RF power with simultaneous modulation of the light intensity obtained for atomic cells #2-5. Each curve is shifted along the vertical axis by the corresponding value of the BG shift (column 4 in Table 1). The vicinities of the zero light shift points are marked by circles. The inset shows the HWHM of the optical lines dependence on the total BG pressure. These values were obtained using mathematical approximation of the absorption line. (b) VCSEL spectra that provide the zero light shift for the atomic cell #2.

4. Discussion

The theoretical model considered in the section 2 is simplified compared with the experimental conditions. The hyperfine structure of the excited state is not taken into account; the medium is assumed to be optically thin, while the absorption level of the resonant sidebands is greater than 30% in the experiment; the spectrum of the considered in the theory phase-modulated optical field (1) does not correspond to the spectrum resulting from the modulation of the VCSEL injection current. While the frequency interval between the spectrum components k and $k + 1$ of the modulated VCSEL is equal to the modulation frequency Ω, the amplitudes of spectrum components can not be described by the Bessel functions $J_k(a)$ and $J_{k+1}(a)$ with reasonable accuracy. In particular, neither the carrier amplitude nor the amplitudes of the first-order sidebands vanish at any available RF power used to modulate the VCSEL injection current; amplitudes of the sidebands $-k$ and k ($k \neq 0$) are not equal to each other, excluding the case when they are equal to zero at a low value of the RF modulation power.

Optics EXPRESS

But in spite of these differences the theoretical calculation is in a qualitative agreement with the experimental results, namely: the index a value (theory) and the RF power value (experiment) corresponding to the first point of the zero light shift increase with growth of the BG pressure, while for the second point of the zero light shift the situation is the opposite; moreover, the value of a and the RF power corresponding to the first point change more quickly than for the second point, see Fig. 1, Fig. 4, and two right columns in Table 1; at a certain value of the total BG pressure these two points merge into one.

This agreement is due to the fact that the light shift induced by higher-order sidebands ($|k| \geq 2$) less effectively compensates the light shift induced by components $k = 0, \mp 1$ with growth of the BG pressure. Furthermore, the light shift from each higher-order sideband even changes in sign with BG pressure, see the formula (4). Therefore, the merging inevitably occurs, regardless of whether the medium is optically thin or thick and how high is a VCSEL modulation efficiency, i.e., how much of the radiation intensity can be concentrated in the higher-order sidebands. Only a certain value of the BG pressure at which the zero light shift points merge into one depends on these factors.

There are two divergences between the theory and the experimental results. First, the observed value of the optical lines broadening, at which merging occurs, is noticeably smaller than the theoretical value: 1.68 GHz (experiment) against 2.92 GHz (theory). This can be explained as follows. The amplitude of the VCSEL carrier does not vanish at any RF power. It increases the higher components ($|k| \geq 2$) power required to compensate the light shift induced by lower components ($k = 0, \mp 1$). But with BG pressure growth this compensation becomes less effective. Therefore, the obtained BG pressure value corresponding to the merging is less than in the theory. Second, the frequencies of the zero light shift points differ by 2-8 Hz, while in theory they are equal. This discrepancy could be caused by the facts that in the experiment we observe the CPT resonance in optically thick medium and the laser spectra corresponding to the zero light shift points are different (see Fig. 4(b)). The resonance's width and asymmetry are also different for this points. All these factors could be the cause of inequality of the frequencies corresponding to the zero light shift points.

The decoherence rate Γ_c in the case of cylindrical geometry of atomic cells can be estimated via the following expression [11,13],

$$\Gamma_c = A \cdot \left[(2.405/D)^2 + (\pi/L)^2\right] / P + B \cdot P, \tag{5}$$

where P is the BG pressure; D and L are diameter and length of an atomic cell, respectively; A and B are parameters depending on alkali metal atoms and the BG used in the atomic cell. The right-hand side of the formula (5) describes the decoherence due to collisions of alkali metal atoms with walls of the cell (the first term), and with the BG (the second term). The optimal value of BG pressure, P_{opt}, which provides the lowest decoherence rate Γ_c, is determined by a simple condition of the equality of the first term to the second term.

Here we point out a way to evaluate the critical size of an atomic cell, at which the value of P_{opt} is equal to P_{merge}, corresponding to merging of the zero light shift points. For a fixed ratio of the length to diameter, the P_{opt} value is inversely proportional to the linear size of the atomic cell or to the cubic root of its volume. Therefore the critical atomic cell size can be estimated as follows. For a cell of a given geometry and size the value of P_{opt} should be obtained experimentally. Its size multiplied by the ratio of P_{opt}/P_{merge} will be critical for atomic cells of the same geometry filled by the same alkali metal atoms and BG.

For the atomic cells used in the experiment the P_{opt} value was found to be nearly 80 Torr and the P_{merge} value was found to be close to 120 Torr. The P_{opt} value was obtained from an experiment in which the same cells with a pressure of 5 to 230 Torr were used. Therefore, the critical size for the atomic cells of the same geometry can be estimated as 5.6 ± 0.8 mm and 10.3 ± 1.5 mm for diameter and length, respectively (taking into account the walls thickness of

Optics EXPRESS

0.7 mm). In the atomic cells of smaller size the lowest decoherence rate Γ_c and the zero light shift can not be obtained simultaneously.

Depending on the chosen value of the total BG pressure, two techniques for the light shift suppression can be implemented in the CPT-based microwave frequency standards. The first technique involves using an atomic cell with low BG pressure at which two points of the zero light shift are easily distinguished. In this case the RF modulation power can be stabilized by means of a feedback loop utilizing modulation of the total optical field intensity [17]. The spectrum corresponding to the first point of the zero light shift is selected. We propose another technique involving the use of BG pressure equal to P_{merge}. In this case, the spectrum corresponding to the minimum of the CPT resonance frequency dependence on the RF power also provides the zero light shift. Therefore, the required feedback loop can be realized by means of modulating the RF power. Even initial tuning the RF power to this value allows to significantly reduce the light shift .

The advantage of the first technique is that the RF power required for the light shift suppression is less than in the second one. It means that there is more optical power in the first-order sidebands and the signal-to-noise ratio is greater. In addition, the CPT resonance frequency is less sensitive to temperature changes at lower BG pressure. However, the second technique may be the only way to achieve an optimum between the Γ_c value and the magnitude of the light shift in miniature atomic cells. Also, this technique does not require additional elements, such as acousto-, electro-optic or liquid-crystal modulator, which increase the device's size and energy consumption.

5. Conclusion

We have demonstrated how dependence of the light shift of the CPT resonance frequency on the RF modulation power of the VCSEL current transforms with increase of the BG pressure. The minimal RF power required for the light shift suppression grows with increase of the total pressure. When a pressure value P_{merge} is reached, two points of the zero light shift merge into one. At higher pressure the light shift value is greater than zero at any spectrum of the RF modulated VCSEL. The case when value of the BG pressure is equal to P_{merge} is suitable for the CPT-based atomic clocks, since the spectrum providing the zero light shift can be controlled by means of a feedback loop realized via modulation of the RF power. A way for estimation of the critical atomic cell size, at which the BG pressure of P_{merge} provides the lowest decoherence rate, is outlined. In atomic cells of smaller dimensions the zero light shift and the lowest decoherence rate can not be obtained simultaneously.

Funding

Russian Science Foundation (19-12-00417).

Acknowledgments

The atomic cells were provided by Atomiks Ltd.

Disclosures

The authors declare no conflicts of interest.

References

1. G. Alzetta, A. Gozzini, L. Moi, and G. Orriols, "An experimental method for the observation of r.f. transitions and laser beat resonances in oriented Na vapour," Nuov. Cim. B **36**(1), 5–20 (1976).
2. R. M. Whitley and C. R. Stroud, "Double optical resonance," Phys. Rev. A **14**(4), 1498–1513 (1976).
3. E. Arimondo and G. Orriols, "Nonabsorbing atomic coherences by coherent two-photon transitions in a three-level optical pumping," Lett. Nuovo Cimento **17**(10), 333–338 (1976).

Optics EXPRESS

4. H. R. Gray, R. M. Whitley, and C. R. Stroud, "Coherent trapping of atomic populations," Opt. Lett. **3**(6), 218–220 (1978).
5. S. Knappe, V. Shah, P. D. D. Schwindt, L. Hollberg, J. Kitching, L. Liew, and J. Moreland, "A microfabricated atomic clock," Appl. Phys. Lett. **85**(9), 1460–1462 (2004).
6. S. Knappe, P. Schwindt, V. Shah, L. Hollberg, J. Kitching, L. Liew, and J. Moreland, "A chip-scale atomic clock based on ^{87}Rb with improved frequency stability," Opt. Express **13**(4), 1249–1253 (2005).
7. J. Kitching, "Chip-scale atomic devices," Appl. Phys. Rev. **5**(3), 031302 (2018).
8. V. Shah and J. Kitching, "Advances in coherent population trapping for atomic clocks," in *Advances in atomic, molecular, and optical physics*, E. Arimondo, P. Berman, and C. Lin, eds. (Academic Press, 2010), vol. 59, chap. 2, pp. 21–74.
9. S. Knappe, R. Wynands, J. Kitching, and H. G. R. L. Hollberg, "Characterization of coherent population-trapping resonances as atomic frequency references," J. Opt. Soc. Am. B **18**(11), 1545–1553 (2001).
10. J. Vanier, "Atomic clocks based on coherent population trapping: a review," Appl. Phys. B: Lasers Opt. **81**(4), 421–442 (2005).
11. J. Vanier and C. Audoin, *The quantum physics of atomic frequency standards* (A. Hilger, 1989).
12. S. Knappe, L. Hollberg, and J. Kitching, "Dark-line atomic resonances in submillimeter structures," Opt. Lett. **29**(4), 388–390 (2004).
13. J. Kitching, S. Knappe, and L. Hollberg, "Miniature vapor-cell atomic-frequency references," Appl. Phys. Lett. **81**(3), 553–555 (2002).
14. J. Vanier, R. Kunski, N. Cyr, J. Y. Savard, and M. Têtu, "On hyperfine frequency shifts caused by buffer gases: Application to the optically pumped passive rubidium frequency standard," J. Appl. Phys. **53**(8), 5387–5391 (1982).
15. F. Levi, A. Godone, and J. Vanier, "The light shift effect in the coherent population trapping cesium maser," IEEE Trans. Ultrason., Ferroelect., Freq. Contr. **47**(2), 466–470 (2000).
16. M. Zhu and L. S. Cutler, "Theoretical and experimental study of light shift in a CPT-based Rb vapor cell frequency standard," in *Proceedings of 32nd Annual Precise Time and Time Interval (PTTI) Meeting*, Lee A. Breakiron, ed. (United States Naval Observatory, 2001), pp. 311–324.
17. V. Shah, V. Gerginov, P. D. D. Schwindt, S. Knappe, L. Hollberg, and J. Kitching, "Continuous light-shift correction in modulated coherent population trapping clocks," Appl. Phys. Lett. **89**(15), 151124 (2006).
18. E. Mikhailov, T. Horrom, N. Belcher, and I. Novikova, "Performance of a prototype atomic clock based on lin ∥ lin coherent population trapping resonances in Rb atomic vapor," J. Opt. Soc. Am. B **27**(3), 417–422 (2010).
19. R. Boudot, P. Dziuban, M. Hasegawa, R. K. Chutani, S. Galliou, V. Giordano, and C. Gorecki, "Coherent population trapping resonances in Cs–Ne vapor microcells for miniature clocks applications," J. Appl. Phys. **109**(1), 014912 (2011).
20. D. Miletic, C. Affolderbach, M. Hasegawa, R. Boudot, C. Gorecki, and G. Mileti, "AC Stark-shift in CPT-based Cs miniature atomic clocks," Appl. Phys. B: Lasers Opt. **109**(1), 89–97 (2012).
21. M. I. Vaskovskaya, V. V. Vassilev, S. A. Zibrov, V. L. Velichansky, I. V. Akimova, A. P. Bogatov, and A. E. Drakin, "Amplitude/phase modulation and spectrum of the vertical-cavity surface-emitting laser output," Quantum Electron. **47**(9), 835–841 (2017).
22. J. Barrat and C. Cohen-Tannoudji, "Étude du pompage optique dans le formalisme de la matrice densité," J. Phys. Radium **22**(6), 329–336 (1961).
23. R. H. Dicke, "The effect of collisions upon the Doppler width of spectral lines," Phys. Rev. A **89**(2), 472–473 (1953).
24. D. S. Chuchelov, V. V. Vassiliev, M. I. Vaskovskaya, V. L. Velichansky, E. A. Tsygankov, S. A. Zibrov, S. V. Petropavlovsky, and V. P. Yakovlev, "Modulation spectroscopy of coherent population trapping resonance and light shifts," Phys. Scr. **93**(11), 114002 (2018).
25. C. Affolderbach, C. Andreeva, S. Cartaleva, T. Karaulanov, G. Mileti, and D. Slavov, "Light-shift suppression in laser optically pumped vapour-cell atomic frequency standards," Appl. Phys. B: Lasers Opt. **80**(7), 841–848 (2005).